

Optical Measurement of Stem Xylem Vulnerability¹[OPEN]

Timothy J. Brodribb,^{a,2} Marc Carriqui,^b Sylvain Delzon,^c and Christopher Lucani^a

^aSchool of Biology, University of Tasmania, Hobart 7001, Australia

^bDepartment of Biology, Universitat de les Illes Balears, Palma, Illes Balears, Spain

^cBIOGECO, INRA, University of Bordeaux, 33610 Pessac, France

ORCID IDs: 0000-0002-4964-6107 (T.J.B.); 0000-0002-0153-2602 (M.C.); 0000-0003-3442-1711 (S.D.); 0000-0001-8983-3575 (C.L.).

The vulnerability of plant water transport tissues to a loss of function by cavitation during water stress is a key indicator of the survival capabilities of plant species during drought. Quantifying this important metric has been greatly advanced by noninvasive techniques that allow embolisms to be viewed directly in the vascular system. Here, we present a new method for evaluating the spatial and temporal propagation of embolizing bubbles in the stem xylem during imposed water stress. We demonstrate how the optical method, used previously in leaves, can be adapted to measure the xylem vulnerability of stems. Validation of the technique is carried out by measuring the xylem vulnerability of 13 conifers and two short-vesselled angiosperms and comparing the results with measurements made using the cavitrion centrifuge method. Very close agreement between the two methods confirms the reliability of the new optical technique and opens the way to simple, efficient, and reliable assessment of stem vulnerability using standard flatbed scanners, cameras, or microscopes.

In modern tracheophytes, xylem cavitation constitutes a fundamental limitation to the functionality of water transport systems. As a consequence, the ability of species to resist or avoid cavitation forms a primary axis of adaptation and ecological variation among land plants (Xu et al., 2016). However, despite the tremendous ecological and physiological insights that await a detailed understanding of the limits and spread of xylem cavitation in plant species, rapid progress has been limited by technical difficulties. These difficulties are largely associated with replicating, under experimental conditions, the metastable hydraulic environment that characterizes water flowing in the xylem when exposed to the large tensions that exist during rapid transpiration or soil water deficit (Cochard et al., 2013).

Most traditional methods of quantifying the degree of xylem embolism require the excision of plant parts (stems, roots, or leaves), causing air or exogenous water to be sucked rapidly into the vasculature, thereby

substantially perturbing the vascular system prior to measurement (Ennajeh et al., 2011; Rockwell et al., 2014). A substantial advance in recent years has been the use of imaging technology that allows water to be viewed inside intact plants, revealing the location and formation of embolisms inside stems (Brodersen et al., 2013), roots (Cuneo et al., 2016), leaves (Bouche et al., 2016; Brodribb et al., 2016a; Scoffoni et al., 2017), and flowers (Zhang and Brodribb, 2017). These studies have substantially changed our view of xylem cavitation and repair, indicating that cavitation can propagate quickly between plant organs (Skelton et al., 2017) and that air blockages (embolisms) are not repaired rapidly in trees after rewatering (Charrier et al., 2016; Choat et al., 2016). Cavitation is now widely viewed as long-term damage to the water transport system of trees that occurs under significant water stress and that is repaired by the regrowth of new xylem tissue (Brodribb et al., 2010; Cochard and Delzon, 2013).

Imaging with x-ray provides unrivaled spatial information about where cavitation occurs in stems and can be used to determine the vulnerability of xylem to cavitation in plant species (Choat et al., 2016; Nolf et al., 2017). However, the damaging nature of the x-ray beam means that high-frequency imaging during the hours and days required to dehydrate plants to water stresses sufficient to cause cavitation is not possible. MRI, on the other hand, can provide spatial and temporal information about cavitation, but low image resolution (pixel sizes larger than the vessels of most species) means that MRI can only be used to resolve embolisms in species with very large vessels. Both techniques require large and expensive hardware and are not currently usable in the field, thus having limited application for measuring large sample sizes. An alternative to these hardware-intensive methods was developed recently using an

¹ This work was supported by the Australian Research Council (grant DP170100761 to T.J.B.) and by a Postgraduate Award to C.L.; M.C. received a travel grant from La Caixa Banking Foundation and from the Conselleria d'Educació, Cultura i Universitats (Govern de les Illes Balears), and a European Social Fund predoctoral fellowship (FPI/1700/2014).

² Address correspondence to timothyb@utas.edu.au.

The author responsible for distribution of materials integral to the findings presented in this article in accordance with the policy described in the Instructions for Authors (www.plantphysiol.org) is: Timothy J. Brodribb (timothyb@utas.edu.au).

T.J.B. conceived the original research plans; T.J.B. and S.D. supervised the experiments; M.C., S.D., C.L., and T.J.B. performed most of the experiments.

[OPEN] Articles can be viewed without a subscription.

www.plantphysiol.org/cgi/doi/10.1104/pp.17.00552

optical technique that measures changes in visual light transmission caused by cavitation in leaf veins (Brodribb et al., 2016a, 2016b). This technique was developed following observations of cavitation bubbles in excised conifer tracheids (Ponomarenko et al., 2014) and provides detailed information about the spatial and temporal evolution of cavitation in the venation network of leaves exposed to water stress. The calculated vulnerability of leaf xylem to cavitation (expressed as P_{50} or water potential required to deactivate 50% of xylem function) using this optical vulnerability (OV) method agrees closely with hydraulically measured P_{50} in leaves (Brodribb et al., 2016b), indicating the utility of the method for quantifying hydraulic failure. Importantly, the OV method requires only a flatbed scanner or camera to collect vulnerability information, thus providing a cost-effective and portable means of assessing leaf xylem vulnerability.

Although the OV method has a demonstrated capacity to reveal leaf vulnerability to water stress, one of the primary applications of xylem cavitation

physiology is in the prediction of tree mortality (Andregg et al., 2015) and species distribution (Larter et al., 2017), and in these applications, stem vulnerability may provide a more definitive mortality threshold than leaves. Studies of potted plants have shown that failure of the stem xylem corresponds closely to the point of tree mortality during acute drought stress (Brodribb and Cochard, 2009; Urli et al., 2013), as might be expected considering the fact that embolism of the stem effectively isolates the leaves from soil water. A vulnerability gradient from stems to leaves is evident in some species (Tyree et al., 1993), but probably not in herbs (Skelton et al., 2017), and it is hypothesized to be a way that woody plants protect their more energy-expensive stem investment by sacrificing leaves during extreme drought (Zimmermann, 1983; Hochberg et al., 2017). Given the importance of understanding stem vulnerability in woody plants, we sought here to extend the highly efficient OV method in leaves to stems. We postulated that the same principle used to identify cavitation in leaves, recording changes in light

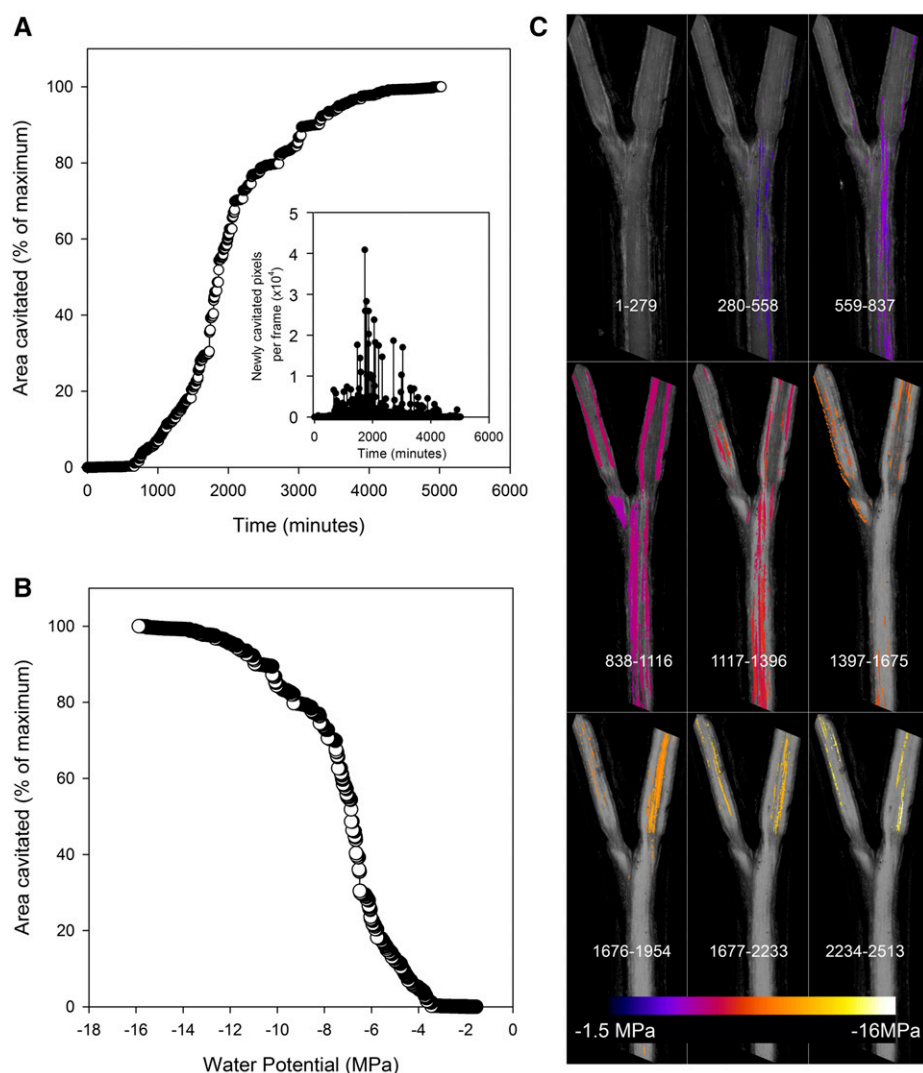


Figure 1. A, A cumulative area of cavitated xylem in a sample stem of *Callitris rhomboidea* is shown to increase rapidly approximately 1 d after a hydrated branch was excised (time zero) and allowed to dry. After a rapid rise in cavitation, the rate of new xylem cavitated (quantified as the number of pixels) falls back to zero approximately 3 d after excision. The inset graph shows that the size of newly cavitated regions visualized in the stem reaches a maximum during the steepest part of the curve. During this period, very large blocks of tracheids were cavitating in the 2-min interval between scans. B, A cumulative area of cavitated xylem expressed as a function of stem water potential shows a classic sigmoidal vulnerability curve. C, A mosaic of color maps shows the spatial progression of cavitation through time in this 20-mm-long branched sample, the same stem sample as in A and B. Sequential blocks of 280 images have been stacked together (frame numbers are shown at the bottom portion of each tile), with cavitated pixels colored according to the water potential at which cavitation occurred. In this sample, the smaller branches proved to be slightly more resistant to cavitation than the main branch.

transmission caused by a transition from liquid- to air-filled xylem conduits during cavitation, could be used in stems. Indeed, it has been known for a long time that air bubbles can be visualized in stems by light microscopy (Vesque, 1883), and this principle was used 80 years ago as a way of identifying the presence of water or air in branches by the evolution of light-colored streaks in the wood after it had been pricked with a sharp scalpel (Haines, 1935). Here, we utilize the principal that a transition from a water-containing to an air-filled conduit during cavitation will cause a distinct color change in visible conduits, from translucent (typically dark) to reflective (white) tissue. Thus, we quantify spatially discrete changes in the refractive index of the stem. Continuous observation of drying stems should thus allow the timing and pattern of cavitation to be recorded and quantified in relation to concurrent measurements of stem water potential.

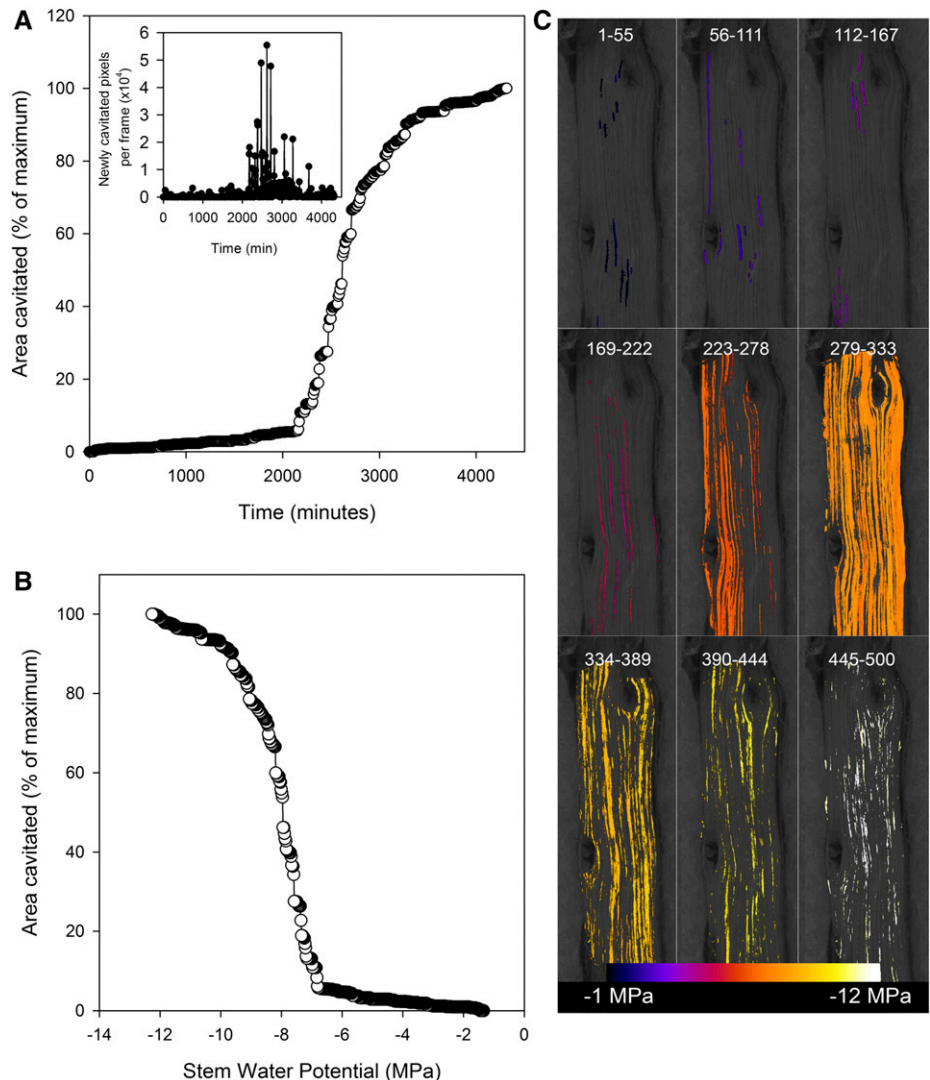
In order to cross validate the new stem optical method, we use a traditional hydraulic centrifuge method as a standard reference for comparison. The

centrifuge method has long been considered an accurate method for assessing xylem vulnerability, except in cases where maximum vessel lengths are similar to the diameter of the centrifuge rotor (Cochard et al., 2013). For this reason, we focused on a diverse group of conifers that lack long xylem conduits, while two short-vessel angiosperms were included to maximize the breadth of the species sample.

RESULTS

Cavitation was easily resolved visually and could be readily quantified by applying image difference to distinguish fast changes in light reflection due to xylem cavitation from slow movements associated with branch deformation during drying. The onset of cavitation was recorded on average 1,308 min after branch excision but ranged from 420 to 2,230 min. In all species, the cumulative total of cavitations recorded followed an approximately sigmoidal function, although this

Figure 2. Similar plots to those in Figure 1 showing the progression of cavitation in a stem of the angiosperm *Rosmarinus officinalis*. Despite the extreme resistance to cavitation in this stem, the vulnerability curve shows a very steep transition from 12% to 88% cavitation. The reason for this steep transition can be seen clearly as due to a number of large and long cavitations between frames 279 and 333.



was never a completely smooth function, typically being punctuated by blocks of major cavitation (Figs. 1 and 2). These blocks of cavitation, often involving hundreds of tracheids in the conifers, typically became larger as water potential approached P_{50} , before diminishing in size toward the end of the drying process. Typically, many cavitation events were recorded in the same part of the stem due to the multiple layers of overlaying xylem that were represented in the 2D image differences. The total cavitated area was typically 150% to 200% of the 2D area of the exposed stem (due to multiple layers of conduits).

Cavitation in the two species of angiosperms also appeared to involve groups of conduits, particularly during the period of maximum intensity of cavitation around P_{50} (Fig. 2). But smaller events, presumably representing individual conduits, often were observed as early events or as a tail toward the end of the cavitation process (Fig. 2).

Large differences in P_{50} were recorded between species using the optical method, with means ranging from -1.2 MPa in *Retrophyllum comptonii* to -9.1 MPa in *Diselma archeri*. Within-species variation also was significant in many species, reaching a maximum in *D. archeri*, where P_{50} ranged between -6.7 and -11.2 MPa between individuals. On average, the coefficient of variation in P_{50} among replicate branches was 16.2% using the optical method and 9.2% using the cavitrone. Mean slopes of the vulnerability curves for each species (between 12% and 88% loss of function) were correlated between the two methods, but the optical method produced steeper slopes on average (Figs. 3 and 4).

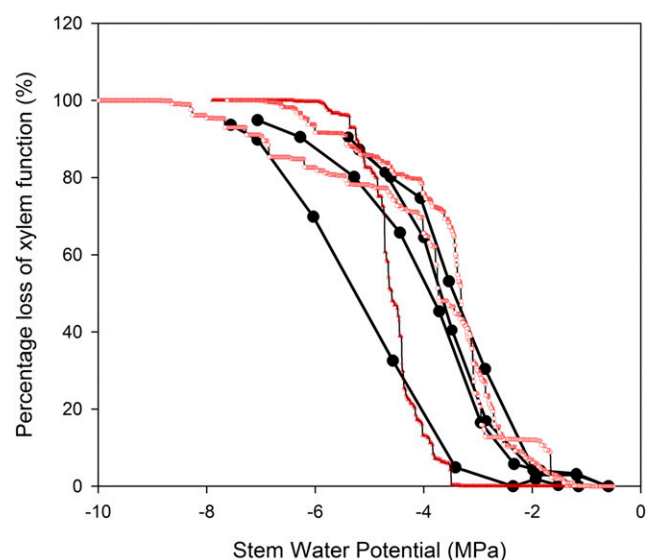


Figure 3. Comparison of the vulnerability curve shape produced by the cavitrone (black circles) and the optical method using branches from the same three individuals of the conifer *Lagarostrobos franklinii*. Although the mean P_{50} is very similar in both species, the slope of the curves between 12% and 88% was steeper using the optical method.

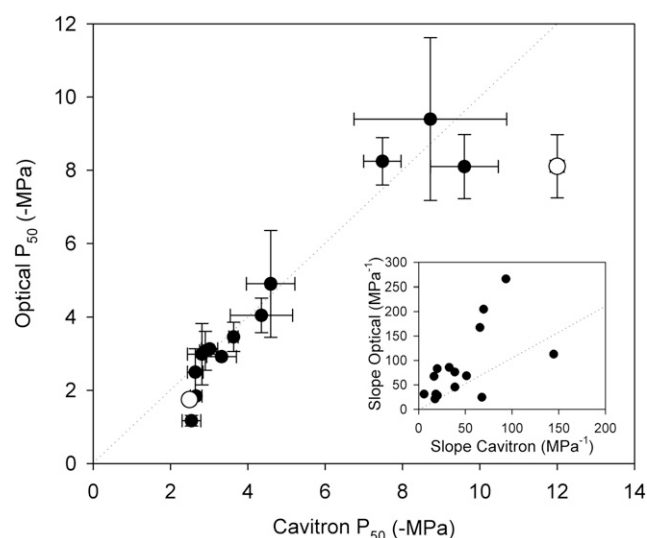


Figure 4. P_{50} (means \pm SD) for stems of the same individuals measured with the optical and cavitrone methods. Very close agreement was found in the conifer sample between methods (regression slope, 0.98; $r^2 = 0.93$). Among the two angiosperms sampled, good agreement was found in one species, while the cavitrone method produced a more negative P_{50} in the second. Slopes produced by the two techniques (inset graph) were correlated ($r^2 = 0.35$; $P < 0.05$), but the optical technique produced a steeper slope in 14 of 16 species (1:1 is shown as a dotted line in each plot).

Among the conifer species, there was strong agreement between P_{50} determined with the optical technique and centrifuge techniques. A regression slope of 0.997 ($r^2 = 0.93$) was found between optical and centrifuge P_{50} in the 13 conifer species, and the ranking of P_{50} was very similar using both methods (Fig. 4).

One of the two angiosperms sampled showed a significant difference between the optical and centrifuge P_{50} . Although both techniques found *R. officinalis* samples to be highly cavitation resistant, P_{50} on the centrifuge (-12 MPa) was 32% more negative than the optical method (-8.1 MPa).

DISCUSSION

A new optical method for visualizing the process of xylem cavitation in plants is shown here to quantify the vulnerability of stem xylem to cavitation-induced reductions in hydraulic function of the stem xylem. The process of cavitation damage to the stem vascular system during water stress could be tracked in time and space on the stems of a diversity of species, including woody conifers and angiosperms. This novel technique represents a very easy and cheap new method for assessing stem vulnerability in woody species using excised branches. In principle, the method also can be used on attached branches, although this was not tested here.

The optical technique allows direct visualization of the process of cavitation in stems under realistic conditions of plant desiccation (as opposed to centrifugation or

stem pressurization). Apart from its simplicity, the advantage of this technique is that it provides a complete view of the spatial and temporal progression of cavitation in stems during increasing water stress. This new perspective on stem cavitation means that continuous monitoring of stem cavitation is possible as bubbles propagate axially in the stem during the development of increasing water deficit. Although cross validation of the technique was performed using woody stems, the technique also works well in herbaceous species, where more translucent stems often do not require phloem removal.

The precisely resolved temporal dynamics of stem cavitation in both conifers and angiosperms studied here all yielded vulnerability curves that were highly sigmoidal in shape, characterized by an initial, extended period of stem desiccation before any stem cavitation events were recorded. This sigmoidal form of xylem vulnerability measured by the OV technique closely matches the form of cavitron (Lamy et al., 2011) and x-ray computed tomography (Choat et al., 2016) vulnerability curves. The majority of data collected using traditional bench drying methods of measuring xylem vulnerability also produce sigmoidal vulnerability curves, but more linear curves often are reported in species with highly stress-resistant xylem (Markesteijn et al., 2011; Vinya et al., 2013). One important benefit of the OV and computed tomography methods of assessing vulnerability is that they report the responses of functioning xylem without reference to a flushed condition. The flushing procedure is required by other hydraulic techniques, whereby samples are subjected to high water pressure to fill all air spaces in the sample and provide a theoretical maximum conductance. Flushing has the potential to activate (refill) xylem that was non-functional in the intact plant, as well as to introduce bubble nuclei, both of which can produce erroneous vulnerability curves (Rockwell et al., 2014).

Among the range of alternative methods for measuring xylem vulnerability, the cavitron was selected here as a standard for comparison because it is considered to be highly reliable when used to measure species with short conduits such as conifers (Cochard et al., 2013). For this reason, most of our sample set was taken from the conifer clade, using the same individuals for both optical (sampled in 2016) and cavitron (sampled in 2012) techniques. The accuracy of centrifuges for measuring angiosperm xylem vulnerability is the subject of considerable debate due to probable artifacts associated with long vessels (Torres-Ruiz et al., 2014; Hacke et al., 2015). For this reason, we only measured two species of angiosperms, selected to cover a range of sensitivities to water stress but both of which had maximum xylem vessel lengths that were approximately half that of the rotor diameter. Despite the huge difference in vulnerability between the two angiosperms measured here, both were found to produce a sigmoidal form in their vulnerability curves using both optical and cavitron methods. Our predawn sampling of well-watered trees ensured that sampled branches started drying from water potentials close to zero, thus

ensuring a minimum of native embolism in the measured samples.

The optical method assesses the loss in xylem function in terms of a cumulative area of stem cavitated in each frame of image sequences. This area-based calculation does not account for the profound influence of xylem conduit radius, in the order of r^4 , that should determine the flow penalty incurred by the cavitation of any particular conduit in the stem (Sperry et al., 2006). Despite this apparent limitation, there was very strong agreement in P_{50} between the optical method (reporting the area of cavitated conduits) and the centrifuge method (quantifying losses in hydraulic conductance). The explanation for the strong agreement between techniques despite different metrics of cavitation is clearly evident from the spatiotemporal distribution of cavitation in stems observed here. Most significant is the evolution of cavitation in large blocks of connected conduits as opposed to discrete conduits, particularly as stems approached the P_{50} water potential. These large interconnected cavitation events also are seen in x-ray images of stems (Choat et al., 2015) and produce a steep slope in the vulnerability curve around P_{50} . Assuming that cavitation in stems on the centrifuge also proceeds in this fashion, it would be expected that the P_{50} values produced by the two techniques would agree. The optical technique emphasizes the importance of connections between conduits more than the size of individual vessels, and due to the nature of cavitation propagation, this is likely to accurately capture the dynamics of flow restriction. Although the slopes of vulnerability curves produced by the cavitron tended to be shallower than those using the optical method, this may be explained by the smaller diameter branches used in the optical versus cavitron technique. Small-diameter (3–6 mm) branches were used for the optical measurements to ensure that cavitations could be visualized from all depths in the stem. Larger diameter stem samples used in the cavitron measurements are likely to incorporate more than one year of growth in the sampled branch, particularly

Table 1. Species list

Species	Family	Class
<i>Agathis robusta</i>	Araucariaceae	Conifer
<i>Araucaria bidwillii</i>	Araucariaceae	Conifer
<i>Araucaria cunninghamii</i>	Araucariaceae	Conifer
<i>Wollemia nobilis</i>	Araucariaceae	Conifer
<i>Callitris rhomboidea</i>	Cupressaceae	Conifer
<i>Diselma archeri</i>	Cupressaceae	Conifer
<i>Acmopyle pancheri</i>	Podocarpaceae	Conifer
<i>Afrocarpus falcatus</i>	Podocarpaceae	Conifer
<i>Dacrycarpus imbricatus</i>	Podocarpaceae	Conifer
<i>Lagarostrobos franklinii</i>	Podocarpaceae	Conifer
<i>Phyllocladus aspleniifolius</i>	Podocarpaceae	Conifer
<i>Prumnopitys ladei</i>	Podocarpaceae	Conifer
<i>Retrophyllum comptonii</i>	Podocarpaceae	Conifer
<i>Retrophyllum rospigliosii</i>	Podocarpaceae	Conifer
<i>Betula pendula</i>	Betulaceae	Angiosperm
<i>Rosmarinus officinalis</i>	Lamiaceae	Angiosperm

considering the slow growth of many of the conifer species used here for comparison. Thus, the cavitron curves reflect the integrated vulnerability of a much larger sample of tracheids than the less than 1-year-old stems measured by the optical method, likely leading to a shallower slope (Torres-Ruiz et al., 2016).

A significant discrepancy between P_{50} in optical and centrifuge methods was only observed in stems of the angiosperm *R. officinalis*. Although both methods recorded extremely high cavitation resistance in this species, the cavitron produced a more negative P_{50} . Further examination of this species and other highly resistant angiosperms will be needed to determine whether this disagreement is due to artifacts or some systematic bias of one of the two methods. One possible contributing factor is the long travel time from Hobart, Australia, to France prior to measurement of this individual. Samples of the same species measured locally with the cavitron yielded values much closer to the OV value (H. Cochard, personal communication). This very resistant end of the vulnerability spectrum is of particular interest, as it appears as a critical adaptation in both conifer (Brodrribb et al., 2014; Larter et al., 2017) and angiosperm (Blackman et al., 2012) tree species inhabiting semiarid woodland.

The success of the optical method in providing a time-resolved map of cavitation in water-stressed stems, while yielding an accurate measure of vulnerability in terms of P_{50} , opens the door to new applications. The simplicity and low cost of the technique make it highly appealing for ecological and genetic research where large sample sizes are required. In addition, the technique provides a means of viewing cavitation in tissues that have been difficult to measure. Flowers have recently been measured successfully using the optical method to show embolism relative to leaves in herbs and woody species (Zhang and Brodrribb, 2017), while roots present an obvious future target. The optical method is ideally suited to explore how cavitation moves within and between plant tissues as water stress intensifies and has the potential to provide an integrated view of cavitation in major plant organs as cavitation propagates within an individual.

MATERIALS AND METHODS

Plant Material

Thirteen species of conifers from four conifer families (Table I) were sampled from a potted conifer collection growing in glasshouses at the University of Tasmania. All plants were more than 10 years old and were growing in 20-L pots under well-watered conditions in partially open glasshouses such that light and temperature were close to ambient conditions in Hobart. Samples for centrifuge analysis were collected and measured in 2012, while samples for optical analysis were collected in 2016 on the same individuals or clones. All species were represented by three replicates collected as cuttings from different individuals in the wild or wild-collected seeds. In addition, we collected two angiosperms with contrasting water stress tolerance to represent opposite ends of the angiosperm vulnerability spectrum but that had relatively short vessels such that they could be measured using the centrifuge technique. These two species (*Rosmarinus officinalis* and *Betula pendula*) were both collected at the end of a wet spring (2016) from single garden plants in Hobart.

Cavitron Stem Vulnerability

Measurements were carried out on one or two branches from three trees per species. Transpiration losses were prevented by removing the needles or leaves immediately after sampling and wrapping the branches in moist paper to keep them humid and cool (5°C) until the measurement of embolism resistance (within 3 weeks of sampling). All samples were sent via an international express shipping company to France within 3 d. Vulnerability to drought-induced embolism was then determined at the Caviplace (University of Bordeaux, Talence, France; <http://sylvain-delzon.com/caviplace>) with the cavitron technique (Cochard, 2002; Cochard et al., 2005). The bark was removed from conifer branches before sampling, to prevent resin contamination, and all branches were recut with a razor blade, under water, to a standard length of 0.27 m. The percentage loss of conductance (PLC) was determined at different speeds (i.e. different xylem pressures) to obtain a vulnerability curve for each sample. These vulnerability curves show the percentage loss of xylem conductance as a function of xylem pressure (for details, see Delzon et al., 2010). For each branch, the relationship between percentage loss of conductance and xylem water pressure was fitted with the following sigmoidal equation (Pammenter and Vander Willigen, 1998):

$$PLC = \frac{100}{\left(1 + \exp\left(\frac{S}{25(P_i - P_{50})}\right)\right)}$$

where P_{50} (MPa) is the xylem pressure inducing a 50% loss of conductivity and S (% MPa⁻¹) is the slope of the vulnerability curve at the inflection point. Mean values of embolism vulnerability parameters (P_{50} and S) correspond to the average values of three to 16 samples per species. Additionally, we used our vulnerability curves to calculate P12 and P88, which are the 12% and 88% loss of hydraulic conductivity, respectively. P12 and P88 are physiologically significant indexes because they are thought to reflect the initial air-entry tension producing embolisms and the irreversible death-inducing xylem tension, respectively (Urli et al., 2013).

Optical Stem Vulnerability

The same individuals or clones of trees collected in 2012 for cavitron determination of P_{50} were revisited and sampled using the OV method. Branches on the order of 1 m long were cut from trees early in the morning and transferred in plastic bags to the laboratory about 50 m away. Branches were generally allowed to equilibrate in moist plastic bags in the dark for a period of 60 min to ensure that stomata were closed before preparing the stem for imaging. The optical method cannot quantify existing embolism in the wood and is only able to measure new cavitations. For this reason, great care was taken to ensure that samples were not exposed to any form of water stress or freezing in the months before measurement.

A stem psychrometer (ICT Australia) was fitted as close as possible to the region of stem being scanned for embolism formation. In fitting the psychrometer, a small square of bark was removed, avoiding damage to the wood. The psychrometer was partially insulated with polystyrene and set to log leaf water potential every 10 min. The cooling time for the psychrometer was increased from 5 to 30 s as stems dried, ensuring a stable reading of the wet-bulb temperature. Reference leaf water potentials were taken during the drying period using a Scholander pressure chamber to ensure that leaf and stem water potentials were equilibrated, as would be expected due to stomatal closure prior to the commencement of cavitation (Brodrribb and Holbrook, 2003). However, after stem cavitation had begun, Scholander and psychrometer values often tended to diverge, as would be expected due to hydraulic disconnection between leaves and stems.

A stem approximately 3 to 6 mm in diameter and approximately 80 to 120 cm in length for conifers, or 1 to 2 m in length for the angiosperms, was selected for scanning. Branches that were actively elongating or expanding leaves were avoided to be sure that the xylem was mature (nonliving). The depth of xylem that could be reliably visualized for cavitation was approximately 1 mm, so a selection of stems were sectioned beforehand to determine the approximate branch thickness that would yield 1 mm of xylem above the pith. A leafless region of the stem, approximately 15 mm in length, was prepared so that xylem on one side of the pith could be imaged. A region of bark approximately 15 to 20 mm in length was carefully removed from one side of the stem to expose the underlying wood without causing damage to the xylem. The easiest way of doing this was to run two parallel axial cuts along the bark on either side of the desired window, avoiding damage to the underlying xylem, and to use a needle or fingernails to peel the bark gently back from the cuts. Once a window was created, it was firmly

secured either onto a flatbed scanner (Perfection 800; Epson) or a microscope stage (Leica M205) using padded clamps to ensure no movement of the sample during drying. Once secured, the scanner or camera was set to capture images at a rate of one per minute, and the sample was left to dry slowly until cavitations were no longer recorded (typically in the order of 48–120 h). During drying, the target region of the stem was mostly darkened except for the light of the microscope (a ring illumination using LED lighting) or scanner. The rest of the stem was exposed to laboratory lighting and ambient conditions of 22°C and 55% relative humidity. In the case of the scanner, images were collected in normal reflective mode rather than the transmission mode used for leaves. Samples were allowed to dry until no further cavitations could be seen in the xylem for a period of 12 h. In some samples, a thin layer of hydrogel (Tensile Gel; Parker) was applied to the exposed xylem surface to improve light transmission and reduce evaporation from the surface. This had no appreciable effect on the value of P_{50} when compared between samples (T.J. Brodrribb, unpublished data), but care was necessary to avoid reflections of movements as the gel shrinks during the drying process.

Once completed, image sequences were analyzed to identify cavitation, which was easily seen as changes in the reflection of the exposed xylem. Analysis by image difference using ImageJ (NIH) was carried out by subtracting successive images to reveal fast changes in contrast produced by cavitation. These rapid changes were easily identified in image subtractions and could be filtered from slow movements caused by drying. Thresholding of image differences allowed automated counting of cavitation events using the analyze-stack function in ImageJ. Full details, including an overview of the technique, image processing, as well as scripts to guide image capture and analysis, are available at <http://www.opensourcecov.org>.

A time-resolved count of cavitations in each stem, quantified as the number of pixels per event during stem drying, was compiled, and this was converted to a percentage of total pixels cavitated. The psychrometer output was then used to determine a fitted function that described the change in stem water potential over time. Typically, this was a linear function once stomata were closed, but occasionally, polynomial functions were fitted to account for variation in the slope $d\psi_{stem}/dt$. Combining the cavitation count with the function describing $d\psi_{stem}/dt$ allowed the cumulative number of cavitations to be expressed as a function of ψ_{stem} . The P_{50} for each sample stem was taken directly from this plot. One value of P_{50} was measured for each of three stems, allowing a mean and SD to be presented for each species.

ACKNOWLEDGMENTS

We thank Tracy Winterbottom and Michelle Lang for the careful maintenance of potted conifers for many years at UTAS.

Received April 21, 2017; accepted June 30, 2017; published July 6, 2017.

LITERATURE CITED

- Anderegg WRL, Flint A, Huang C, Flint L, Berry JA, Davis FW, Sperry JS, Field CB (2015) Tree mortality predicted from drought-induced vascular damage. *Nat Geosci* 8: 367–371
- Blackman CJ, Brodrribb TJ, Jordan GJ (2012) Leaf hydraulic vulnerability influences species' bioclimatic limits in a diverse group of woody angiosperms. *Oecologia* 168: 1–10
- Bouche PS, Delzon S, Choat B, Badel E, Brodrribb TJ, Burrell R, Cochard H, Charra-Vaskou K, Lavigne B, Li S (2016) Are needles of *Pinus pinaster* more vulnerable to xylem embolism than branches? New insights from x-ray computed tomography. *Plant Cell Environ* 39: 860–870
- Brodersen CR, McElrone AJ, Choat B, Lee EF, Shackel KA, Matthews MA (2013) In vivo visualizations of drought-induced embolism spread in *Vitis vinifera*. *Plant Physiol* 161: 1820–1829
- Brodrribb TJ, Bienaimé D, Marmottant P (2016a) Revealing catastrophic failure of leaf networks under stress. *Proc Natl Acad Sci USA* 113: 4865–4869
- Brodrribb TJ, Bowman DJMS, Nichols S, Delzon S, Burrell R (2010) Xylem function and growth rate interact to determine recovery rates after exposure to extreme water deficit. *New Phytol* 188: 533–542
- Brodrribb TJ, Cochard H (2009) Hydraulic failure defines the recovery and point of death in water-stressed conifers. *Plant Physiol* 149: 575–584
- Brodrribb TJ, Holbrook NM (2003) Stomatal closure during leaf dehydration, correlation with other leaf physiological traits. *Plant Physiol* 132: 2166–2173
- Brodrribb TJ, McAdam SA, Jordan GJ, Martins SC (2014) Conifer species adapt to low-rainfall climates by following one of two divergent pathways. *Proc Natl Acad Sci USA* 111: 14489–14493
- Brodrribb TJ, Skelton RP, McAdam SA, Bienaimé D, Lucani CJ, Marmottant P (2016b) Visual quantification of embolism reveals leaf vulnerability to hydraulic failure. *New Phytol* 209: 1403–1409
- Charrier G, Torres-Ruiz JM, Badel E, Burrell R, Choat B, Cochard H, Delmas CE, Domec JC, Jansen S, King A (2016) Evidence for hydraulic vulnerability segmentation and lack of xylem refilling under tension. *Plant Physiol* 172: 1657–1668
- Choat B, Badel E, Burrell R, Delzon S, Cochard H, Jansen S (2016) Non-invasive measurement of vulnerability to drought-induced embolism by x-ray microtomography. *Plant Physiol* 170: 273–282
- Choat B, Brodersen CR, McElrone AJ (2015) Synchrotron x-ray microtomography of xylem embolism in *Sequoia sempervirens* saplings during cycles of drought and recovery. *New Phytol* 205: 1095–1105
- Cochard H (2002) A technique for measuring xylem hydraulic conductance under high negative pressures. *Plant Cell Environ* 25: 815–819
- Cochard H, Badel E, Herbette S, Delzon S, Choat B, Jansen S (2013) Methods for measuring plant vulnerability to cavitation: a critical review. *J Exp Bot* 64: 4779–4791
- Cochard H, Damour G, Bodet C, Tharwat I, Poirier M, Ameglio T (2005) Evaluation of a new centrifuge technique for rapid generation of xylem vulnerability curves. *Physiol Plant* 124: 410–418
- Cochard H, Delzon S (2013) Hydraulic failure and repair are not routine in trees. *Ann For Sci* 70: 659–661
- Cuneo IF, Knipfer T, Brodersen CR, McElrone AJ (2016) Mechanical failure of fine root cortical cells initiates plant hydraulic decline during drought. *Plant Physiol* 172: 1669–1678
- Delzon S, Douthe C, Sala A, Cochard H (2010) Mechanism of water-stress induced cavitation in conifers: bordered pit structure and function support the hypothesis of seal capillary-seeding. *Plant Cell Environ* 33: 2101–2111
- Ennajeh M, Simões F, Khemira H, Cochard H (2011) How reliable is the double-ended pressure sleeve technique for assessing xylem vulnerability to cavitation in woody angiosperms? *Physiol Plant* 142: 205–210
- Hacke UG, Venturas MD, MacKinnon ED, Jacobsen AL, Sperry JS, Pratt RB (2015) The standard centrifuge method accurately measures vulnerability curves of long-vesselled olive stems. *New Phytol* 205: 116–127
- Haines F (1935) Observations on the occurrence of air in conducting tracts. *Ann Bot (Lond)* 49: 367–379
- Hochberg U, Windt CW, Ponomarenko A, Zhang YJ, Gersony J, Rockwell FE, Holbrook NM (2017) Stomatal closure, basal leaf embolism, and shedding protect the hydraulic integrity of grape stems. *Plant Physiol* 174: 764–775
- Lamy JB, Bouffier L, Burrell R, Plomion C, Cochard H, Delzon S (2011) Uniform selection as a primary force reducing population genetic differentiation of cavitation resistance across a species range. *PLoS ONE* 6: e23476
- Larter M, Pfautsch S, Domec JC, Trueba S, Nagalingum N, Delzon S (2017) Aridity drove the evolution of extreme embolism resistance and the radiation of conifer genus *Callitris*. *New Phytol* 215: 97–112
- Markestijn L, Poorter L, Paz H, Sack L, Bongers F (2011) Ecological differentiation in xylem cavitation resistance is associated with stem and leaf structural traits. *Plant Cell Environ* 34: 137–148
- Nolf M, Lopez R, Peters JMR, Flavel RJ, Kolodain LS, Young IM, Choat B (2017) Visualization of xylem embolism by x-ray microtomography: a direct test against hydraulic measurements. *New Phytol* 214: 890–898
- Pammenter NW, Vander Willigen C (1998) A mathematical and statistical analysis of the curves illustrating vulnerability of xylem to cavitation. *Tree Physiol* 18: 589–593
- Ponomarenko A, Vincent O, Pietriga A, Cochard H, Badel É, Marmottant P (2014) Ultrasonic emissions reveal individual cavitation bubbles in water-stressed wood. *J R Soc Interface* 11: 20140480
- Rockwell FE, Wheeler JK, Holbrook NM (2014) Cavitation and its discontents: opportunities for resolving current controversies. *Plant Physiol* 164: 1649–1660
- Scoffoni C, Albuquerque C, Brodersen CR, Townes SV, John GP, Cochard H, Buckley TN, McElrone AJ, Sack L (2017) Leaf vein xylem conduit diameter influences susceptibility to embolism and hydraulic decline. *New Phytol* 213: 1076–1092

- Skelton RP, Brodribb TJ, Choat B** (2017) Casting light on xylem vulnerability in an herbaceous species reveals a lack of segmentation. *New Phytol* **214**: 561–569
- Sperry JS, Hacke UG, Pittermann J** (2006) Size and function in conifer tracheids and angiosperm vessels. *Am J Bot* **93**: 1490–1500
- Torres-Ruiz JM, Cochard H, Mayr S, Beikircher B, Diaz-Espejo A, Rodriguez-Dominguez CM, Badel E, Fernández JE** (2014) Vulnerability to cavitation in *Olea europaea* current-year shoots: further evidence of an open-vessel artifact associated with centrifuge and air-injection techniques. *Physiol Plant* **152**: 465–474
- Torres-Ruiz JM, Cochard H, Mencuccini M, Delzon S, Badel E** (2016) Direct observation and modelling of embolism spread between xylem conduits: a case study in Scots pine. *Plant Cell Environ* **39**: 2774–2785
- Tyree M, Cochard H, Cruiziat P, Sinclair B, Ameglio T** (1993) Drought-induced leaf shedding in walnut: evidence for vulnerability segmentation. *Plant Cell Environ* **16**: 879–882
- Urli M, Porté AJ, Cochard H, Guengant Y, Burlett R, Delzon S** (2013) Xylem embolism threshold for catastrophic hydraulic failure in angiosperm trees. *Tree Physiol* **33**: 672–683
- Vesque J** (1883) Observation directe du mouvement de l'eau dans les vaisseaux des plantes. *Annals de Science Naturelles Botanique* **15**: 5–15
- Vinya R, Malhi Y, Fisher JB, Brown N, Brodribb TJ, Aragao LE** (2013) Xylem cavitation vulnerability influences tree species' habitat preferences in miombo woodlands. *Oecologia* **173**: 711–720
- Xu X, Medvigy D, Powers JS, Becknell JM, Guan K** (2016) Diversity in plant hydraulic traits explains seasonal and inter-annual variations of vegetation dynamics in seasonally dry tropical forests. *New Phytol* **212**: 80–95
- Zhang FP, Brodribb TJ** (2017) Are flowers vulnerable to xylem cavitation during drought? *Proc R Soc B* **284**: 20162642
- Zimmermann MH** (1983) *Xylem Structure and the Ascent of Sap*. Springer-Verlag, Berlin